

Inclusion-Water-Cluster in a Three-Dimensional Superlattice of Gold Nanoparticles

Suhua Wang, Hiroshi Yao, Seiichi Sato, and Keisaku Kimura*

Department of Material Science, Himeji Institute of Technology, 3-2-1 Kohto, Kamigori-cho, Akou-gun, Hyogo 678-1297, Japan

Received December 19, 2003; E-mail: kimura@sci.himeji-tech.ac.jp

Assembling nanoparticles into ordered two-dimensional (2D) and 3D superstructures and investigating their collective properties have recently been receiving much attention.¹ Most of the reported nanoparticles are passivated with a long-chain alkane ligand, commonly hydrophobic in nature. An inherent van der Waals attraction and a hard-sphere repulsion are the driving forces for the particles to assemble orderly. Another candidate is hydrogen bonding by water that plays a crucial role in protein and molecular crystals. Water is included as an essential part of the structure in some cases, such as crystalline water, coordination water, or bound water. Utilization of hydrogen bonding in growing colloidal crystals became possible and practical when the preparation method for hydrophilic nanoparticles from hydrosol was established.² Gold nanoparticles are passivated with a short-chain dicarboxylic acid, mercaptosuccinic acid (MSA), which provides OH groups for the formation of hydrogen bonds. On the basis of the elemental analysis of well-dried particles, stoichiometric inclusion of water molecules was found.³ Well-grown faceted colloidal crystals made of Au–MSA are very stable upon exposure to most polar and nonpolar solvents.^{2,4} We have discovered self-correcting processes and inclusions of water molecules in the crystal during the equilibrium growth.^{4–6} Carboxylic acids tend to form dimers through hydrogen bonding. Therefore, hydrogen bonding among OH groups is presumed to be the force that connects the building gold nanoparticles in the gold-particle crystals.³ OH vibrational stretching modes have relatively high frequencies which are largely isolated from IR bands of other chemical bonds. Hence, the absorption band between 3000 and 3700 cm^{-1} displays a characteristic window for intermolecular hydrogen bonding between OH groups. In this communication, therefore, IR spectroscopy was used to study the interactions among the developing gold nanoparticles within the crystals.

Three reference samples provide fundamental information on the configuration of MSA. The first two references are pure MSA (Figure 1A) and as-prepared gold nanoparticles (sample B). As demonstrated in previous works,^{3,5} MSA in the as-prepared gold nanoparticles without dialysis exist in the form of sodium carboxylate, but as the acid form in particle crystals. Figure 1B is depicted, based on the elemental analysis data for the as-prepared lyophilized powdered sample, showing that the ratio of MSA to H_2O is unity. Figure 1C was proposed on the grounds of the tendency of aggregates to form under humid conditions (The original was depicted for sodium salt).³ Therefore, the third reference, sample C, was protonated nanoparticles. The gold particle crystals (sample D) were produced following the literature method.^{2,5} These crystals reveal well-developed crystal facets (Figure 1D) and hexagonal close packing.⁵

In Figure 2 are shown the FT-IR spectra of samples (A), (B), (C), and (D), and all samples have obvious absorptions in the OH vibrational stretching region. However, the particle crystals have particular features in the band at the highest frequency and three

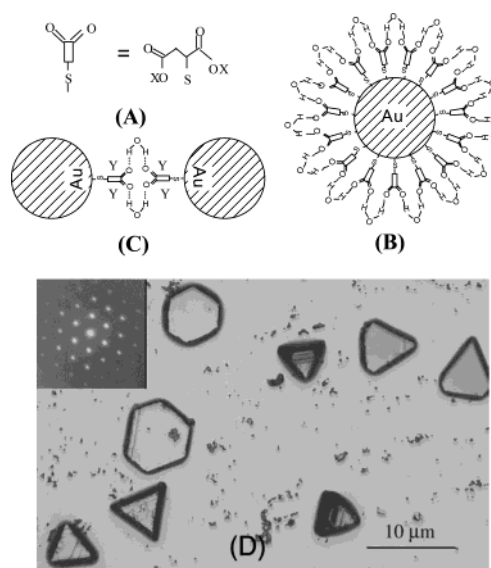


Figure 1. (A) Molecular structure of MSA, in which X denotes H or Na atom. (B) Configuration of MSA on the gold nanoparticle surface that allows one water molecule to connect with two carbonyl groups in the adjoining MSA to make a successive hydrogen-bonding network. (C) One water molecule connects with two carbonyl groups from different particles, which induces aggregation of two particles in a humid condition. Symbol Y stands for a possible spacing for water cluster. (D) Microscope images of gold particle crystals. Inset shows low-angle electron diffraction from one superlattice.

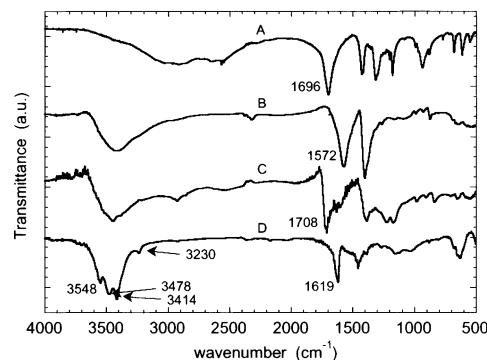


Figure 2. FT-IR spectra: (A) pure MSA molecules, (B) as-prepared gold nanoparticles (sodium salt), (C) protonated gold nanoparticles, and (D) gold colloidal crystals.

well-resolved absorption peaks. There are two sources of OH groups in the gold particle crystals. One is from the carboxylic groups of MSA molecules.³ The other is from water molecules, which are included in the superlattices during the equilibrium growth process. It is well-known that carboxylic acid molecules with no other polar groups usually exist predominantly as the hydrogen-bonded dimer,

which results in a very broad OH stretching band around 3000 cm^{-1} and an asymmetric C=O stretching band at $1740\text{--}1680\text{ cm}^{-1}$.⁷ This is clearly seen in Figure 2A. When MSA bonds to the surface of gold nanoparticles and forms carboxylate during nanoparticle preparation, a water molecule strongly binds to the MSA moiety even in well-dried powders as evidenced by an elemental analysis and by thermogravimetry.³ This bound water molecule can be released above $105\text{ }^{\circ}\text{C}$. The shift of the C=O stretching peak to the low frequency of 1572 cm^{-1} (Figure 2B) is consistent with the formation of carboxylate ion (COO^-).⁸ It is also seen in Figure 2B that the carboxylic OH stretching band around 3000 cm^{-1} disappears and a new poorly resolved broad band appears, centering at 3400 cm^{-1} , which is attributed to water molecules bound to the as-prepared gold nanoparticles. When carboxylic acid molecules exist in the monomeric state, however, the OH stretching vibration absorbs at $3550\text{--}3500\text{ cm}^{-1}$, and the C=O stretching shifts simultaneously to a higher frequency around $1800\text{--}1740\text{ cm}^{-1}$.⁸ The observed C=O stretch peak in Figure 2C is 1708 cm^{-1} , slightly higher than that of pure MSA (1696 cm^{-1}) and lower than that of free carboxylic acid monomer. Observation of a band at around 3000 cm^{-1} and a broad band near 3400 cm^{-1} suggests the water-bound carboxylic acid in Sample C.

The OH symmetric (ν_1) and antisymmetric (ν_3) vibrational stretching fundamentals of the water monomer are at 3650 and 3755 cm^{-1} , respectively.⁷ For liquid water or bound water in many cases, however, the OH stretching band is red-shifted from ν_1 and ν_3 by several hundred wavenumbers due to hydrogen-bonding networks, and the features are completely masked by overwhelming background absorption from distant water molecules.^{7–9} That is, the hydrogen-bonded water molecules in a distributed-bound state result in an unresolved and broad OH band centered at 3400 cm^{-1} . However, for the gold particle crystals having the same chemical composition as in the protonated gold nanoparticle powders for MSA, three well-resolved peaks are detected as in Figure 2D at 3548 , 3478 , and 3414 cm^{-1} , respectively. All positions are about 300 cm^{-1} red-shifted from that of water monomer. The water molecules adsorbed in the as-prepared and protonated gold nanoparticles combine with the carbonyl groups of MSAs through hydrogen bonding.^{3,5} In this case, the OH stretching band of water showed nearly the same spectra as those in Figure 2B or C. Hence, we exclude hydrogen-bonding networks of bulk water or the existence of water monomers in sample D. The presence of 1619 cm^{-1} absorption in the crystals immediately rules out the MSA monomeric state. The low energy-shift of this band implies that the effective mass of C=O stretching is larger than that of the dimeric state of carboxylic acid, i.e. C=O is bound by several hydrogen bonds. Figure 2D shows no OH stretching band around 3000 cm^{-1} , implying that the OH groups of the MSA should not be free but probably bond with water.

We can also rule out the presence of water dimer in the superlattices, because the dimer exhibit OH vibrational peaks at ca. 3710 and ca. 3620 cm^{-1} which are slightly red-shifted to the water monomer bands.¹⁰ On the other hand, water clusters such as $(\text{H}_2\text{O})_n$ ($n = 8\text{--}10$) have been reported to exhibit well-resolved peaks in $3400\text{--}3600\text{ cm}^{-1}$, just falling in the region of the observed splitting IR band.¹¹ Therefore, it is reasonable to presume that the observed three peaks come from interstitial small water clusters, “inclusion-water-clusters” which combine with carboxylic groups through hydrogen-bonding interactions. The formation of hydrogen bonding between MSA molecules and water clusters lowers the

force constant of carboxylic OH bond. This will correspondingly result in a red-shift of the carboxylic OH stretching from $\sim 3520\text{ cm}^{-1}$ of the monomer.⁸ The obvious but relatively weak absorption peak at 3230 cm^{-1} is therefore attributed to the OH vibrational stretching of carboxylic groups in MSA. The approximately 300 cm^{-1} -shift is consistent with that of the OH stretching mode from water.

Although we could not determine the structures of interstitial water clusters from the IR spectra, the formation of water clusters is most probable in the superlattice. In a hexagonal close-packed alignment of surface-modified nanoparticles, a tetrahedral Td or octahedral Oh interstitial cavity is produced along with that between two adjacent nanoparticles. It is plausible that carboxylic groups in MSA combine with water cluster of definite size in the confined cavities through intermolecular hydrogen bonding. That is, water clusters intervene among MSA-modified gold nanoparticles, which stabilize the nanoparticle crystals. The size and structure of the clusters depend on their locations in the superlattice.¹²

In conclusion, we have found the “inclusion-water-cluster” for the first time. The results show that water clusters are trapped in the interstice of superlattices and connect the building gold nanoparticles through hydrogen bonding.

Acknowledgment. Financial support and granting the postdoctoral fellowship (P01261) from the Japan Society for Promotion of Science is gratefully acknowledged. We are indebted to support in part by Grants-in-Aid for Scientific Research (B:13440212) from MEXT and by Mitsubishi Research Institute, Japan Space Utilization Promotion Center and Hyogo Science and Technology Promotion Foundation.

Supporting Information Available: Experimental procedures and TEM and XRD data (PDF). This material is available free of charge via the Internet at <http://pubs.acs.org>.

References

- (1) (a) Weller, H. *Curr. Opin. Colloid Interface Sci.* **1998**, *3*, 194. (b) Collier, C. P.; Vossmeier, T.; Heath, J. R. *Annu. Rev. Phys. Chem.* **1998**, *49*, 371. (c) Murray, C. B.; Kagan, C. R.; Bawendi, M. G. *Annu. Rev. Mater. Sci.* **2000**, *30*, 545. (d) Ohara, P. C.; Heath, J. R.; Gelbart, W. M. *Angew. Chem., Int. Ed. Engl.* **1997**, *36*, 1078. (e) Lin, X. M.; Jaeger, H. M.; Sorensen, C. M.; Klabunde, K. J. *J. Phys. Chem. B* **2001**, *105*, 3353. (f) Giersig, M.; Mulvaney, P. *Langmuir* **1993**, *9*, 3408. (g) Dabbousi, B. O.; Murray, C. B.; Rubner, M. F.; Bawendi, M. G. *Chem. Mater.* **1994**, *6*, 216. (h) Legrand, J.; Petit, C.; Pileni, M. P. *J. Phys. Chem. B* **2001**, *105*, 5643. (i) Harfenist, S. A.; Wang, Z. L.; Whetten, R. L.; Vezmar, I.; Alvarez, M. M. *Adv. Mater.* **1997**, *9*, 817. (j) Courty, A.; Araspin, O.; Fermon, C.; Pileni, M. P. *Langmuir* **2001**, *17*, 1372.
- (2) Kimura, K.; Sato, S.; Yao, H. *Chem. Lett.* **2001**, 372.
- (3) Chen, S.; Kimura, K. *Langmuir* **1999**, *15*, 1075.
- (4) Sato, S.; Yao, H.; Kimura, K. *Physica E* **2003**, *17*, 521.
- (5) (a) Wang, S.; Sato, S.; Kimura, K. *Chem. Mater.* **2003**, *15*, 1075. (b) Stoeva, S. I.; Prasad, B. L. V.; Uma, S.; Stoimenov, P. K.; Zaikovski, V.; Sorensen, C. M.; Klabunde, K. J. *J. Phys. Chem. B* **2003**, *107*, 7441.
- (6) (a) Sato, S.; Yamamoto, H.; Yao, H.; Kimura, K. *Mater. Res. Soc. Symp. Proc.* **2002**, *703*, 375. (b) Wang, S. H.; Sato, S.; Kimura, K. *Chem. Lett.* **2003**, *32*, 520. (c) Yao, H.; Kojima, H.; Sato, S.; Kimura, K. *Chem. Lett.* **2003**, *32*, 698.
- (7) Braun, C. L.; Smirnov, S. N. *J. Chem. Edu.* **1993**, *70*, 612.
- (8) Colthup, N. B.; Daly, L. H.; Wiberley, S. E. *Introduction to Infrared and Raman Spectroscopy*, 3rd ed.; Academic Press: San Diego, CA, 1990; pp 256–260, pp 239–268, p 291.
- (9) Weber, J. M.; Kelley, J. A.; Nielsen, S. B.; Ayotte, P.; Johnson, M. A. *Science* **2000**, *287*, 2461.
- (10) Tursi, A. J.; Nixon, E. R. *J. Chem. Phys.* **1970**, *52*, 1521.
- (11) (a) Buck, U.; Ettischer, I.; Melzer, M.; Buch, V.; Sadlej, J. *Phys. Rev. Lett.* **1998**, *80*, 2578. (b) Jensen, J. O.; Krishnan, P. N.; Burke, L. A. *Chem. Phys. Lett.* **1995**, *246*, 13.
- (12) Relevant lattice parameters from TED are given and discussed in Supporting Information.

JA031822+